

Spectral Modeling of Difference-Frequency Generation in the Case of Two-Frequency Interaction of Ultrasound Waves

A. V. Tyurina^{a, *}, P. V. Yuldashev^{a, **}, I. B. Esipov^b, and V. A. Khokhlova^{a, ***}

^a Faculty of Physics, Moscow State University, Moscow, 119991 Russia

^b Gubkin Russian State University of Oil and Gas, Moscow, 119991 Russia

*e-mail: tiurina.av@physics.msu.ru

**e-mail: petr@acs366.phys.msu.ru

***e-mail: vera@acs366.phys.msu.ru

Received November 3, 2021; revised November 25, 2021; accepted November 30, 2021

Abstract—A spectral algorithm is considered for describing nonlinear generation of an acoustic wave of difference frequency formed as the interaction of two high-intensity pump waves close in frequency. To correctly simulate the full wave spectrum involved in such two-frequency interaction, including formation of shock fronts in the acoustic pressure waveform, it is necessary to retain about several thousand spectral components in the numerical algorithm. This paper proposes a method that enables to significantly reduce this number while maintaining the accuracy of calculating the difference-frequency wave field. The method combines the limitation of the high-frequency part of the spectrum and the combination frequencies located between the spectral components that are multiples of frequencies of the initial pump waves. Examples of the interaction of close frequencies typical for the operation of an underwater parametric array are considered in the approximation of the plane one-dimensional wave propagation. It was shown that the method makes it possible to reduce the number of spectral components included in the nonlinear algorithm by more than 100 times and thereby reduce the number of operations by four orders of magnitude. This makes the algorithms for simulating parametric interactions in ultrasound wave fields feasible, including three-dimensional acoustic beams.

Keywords: nonlinearity, spectral approach, difference frequency

DOI: 10.1134/S1063771022020105

INTRODUCTION

Studying the parametric processes in ultrasound wave interactions is an important problem in practical applications of nonlinear acoustics [1, 2]. During the nonlinear interaction of two high-intensity pump waves with close frequencies f_{pump1} and f_{pump2} , multiple harmonics and combination frequencies are generated. Since absorption in a medium increases with frequency, high-frequency spectral components decay faster, and at distances far from the source, only the wave of the difference frequency $f_{\text{dif}} = |f_{\text{pump1}} - f_{\text{pump2}}|$ propagates [3]. Development of algorithms for simulating a difference-frequency wave field remains an important problem due to a number of advantages of the nonlinear mechanism of generating low-frequency radiation and, as a consequence, the wide practical applications of parametric arrays. An important feature of the two-frequency interaction is an extremely high directivity (on the order of several degrees) of the low-frequency radiation [4, 5]. In addition, in comparison with a conventional sound source operating at the same frequency, a parametric array has a small

size, no sidelobes in the directivity pattern, and a wide frequency bandwidth of the radiated signal.

Parametric arrays have been studied, both theoretically [6] and experimentally, over the past several decades [7–9]. They have been actively used both in underwater acoustics, e.g., for ocean acoustic tomography, ocean sounding, and profiling of bottom structures [4]; and in aeroacoustics [10], e.g., for creating audio spotlights [11] in various practical applications [12].

Theoretical models of varying complexity have been used for governing the generation and propagation of a difference-frequency wave. The most general approach for solving three-dimensional problems is to solve a system of nonlinear equations for a compressible viscous continuous medium using finite-difference methods [13]. However, obtaining the solution of this system even for radially symmetric sources is computationally cumbersome. A more practically suitable model is the one-way Westervelt equation, which takes into account the effects of nonlinearity, diffraction,

and thermoviscous absorption [3]. In the retarded time coordinate system, it can be written as follows:

$$\frac{\partial p}{\partial z} = \frac{\beta}{c_0^3 \rho_0} p \frac{\partial p}{\partial \tau} + \frac{\delta}{2c_0^3} \frac{\partial^2 p}{\partial \tau^2} + \frac{c_0}{2} \int_{-\infty}^{\tau} \Delta p d\tau'. \quad (1)$$

Here, p is the acoustic pressure, z is the propagation coordinate along the beam axis, $\tau = t - z/c_0$ is the retarded time, $\Delta = \partial^2/\partial x^2 + \partial^2/\partial y^2 + \partial^2/\partial z^2$ is the Laplacian, c_0 is the sound speed, ρ_0 is the density of a medium, and β and δ are the nonlinearity and thermoviscous absorption coefficients in the medium, respectively. If necessary, the equation can also take into account other absorption mechanisms, e.g., relaxation.

Originally, the Westervelt equation was used in the modeling of parametric interactions to obtain analytical estimates of the pressure amplitude at difference frequency in the far field of a transducer [3]. In modern studies, the Westervelt equation is solved numerically, for example, by finite-difference methods in the time-domain representation [14]. This equation can also be used to obtain semi-analytical solutions for the difference-frequency field in the quasi-linear approximation without paraxial approximation [15].

For ultrasound sources used in medical acoustics, the Westervelt equation has been widely solved numerically using operator-splitting method [16, 17]. According to this method, at each step along the coordinate of wave propagation, the operators on the right-hand side of the equation describing various physical effects are calculated separately. Such approach makes it possible to use the most effective numerical scheme for each particular operator. The main challenge arises when calculating the diffraction operator, for the implementation of which the angular spectrum method is often used [18]. For parametric sources, such simulation method has been implemented in the quasi-linear approximation for three-dimensional geometry of the acoustic field [19].

A simpler model for calculating the fields of parametric sources is the Khokhlov–Zabolotskaya–Kuznetsov (KZK) equation

$$\frac{\partial p}{\partial z} = \frac{\beta}{c_0^3 \rho_0} p \frac{\partial p}{\partial \tau} + \frac{\delta}{2c_0^3} \frac{\partial^2 p}{\partial \tau^2} + \frac{c_0}{2} \int_{-\infty}^{\tau} \Delta_{\perp} p d\tau', \quad (2)$$

which differs from the Westervelt equation in the use of the paraxial approximation in calculating the diffraction operator in the right-hand side of the equation. Here, $\Delta_{\perp} = \partial^2/\partial x^2 + \partial^2/\partial y^2$ is the Laplacian over the transverse coordinates. The finite-difference numerical schemes have been developed for the KZK equation both in the time- [20] and frequency-domain representations [21]. They are also based on the operator-splitting approach. Later, these schemes were used to describe the difference-frequency fields of radially symmetric [22–24] and rectangular [25] sources.

The main difficulty in modeling parametric interactions in nonlinear beams is as follows. If we do not restrict ourselves to the quasi-linear approximation and take into account the formation of shock fronts in the pump wave, then the number of spectral components that must be formally included in the algorithm becomes very large, on the order of several thousands. This becomes critical when the spectral method is used to calculate a nonlinear operator, since the number of operations is proportional to the number of harmonics squared [26]. In this case, when solving the Eqs. (1) and (2) using operator-splitting scheme, a one-dimensional nonlinear problem is actually solved at each step of the grid along the wave propagation coordinate. The use of time-domain algorithms is also challenging, since, on the one hand, the time window must be sufficiently wide to encompass the low-frequency component, and on the other hand, the time sampling rate must be sufficiently small to correctly represent the high-frequency components and their harmonics. As a result, three-dimensional modeling of parametric processes in acoustic fields created by sources with arbitrary-shaped apertures becomes difficult, both in terms of the required RAM and computation time, even using modern computers with multi-core processors.

This limitation can be overcome by selecting the most essential spectral components that contribute to forming the signal at the difference frequency and retaining only these harmonics in the numerical scheme. This idea has been considered earlier, but as far as we know, it has not been realized [24]. In our study, we propose to optimize the calculation of a nonlinear operator by filtering the wave spectrum and identifying criteria for excluding or retaining the spectral harmonics. The algorithm for solving the Eqs. (1) and (2) in a one-dimensional formulation is presented taking into account only the nonlinearity and absorption operators, and the corresponding parametric phenomena are described. In this case, without account for the diffraction operator, Eqs. (1) and (2) transform into the one-dimensional nonlinear Burgers equation [27]. The proposed method can considerably reduce the number of operations in the algorithm for calculating the nonlinear operator. Development of the method in a one-dimensional formulation is aimed at its further use in solving the complete nonlinear-diffraction problem, consideration of which is beyond the scope of this study.

1. THEORETICAL APPROACH

1.1. Nonlinear Burgers Equation

To model the nonlinear and absorption effects during the interaction of two one-dimensional high-

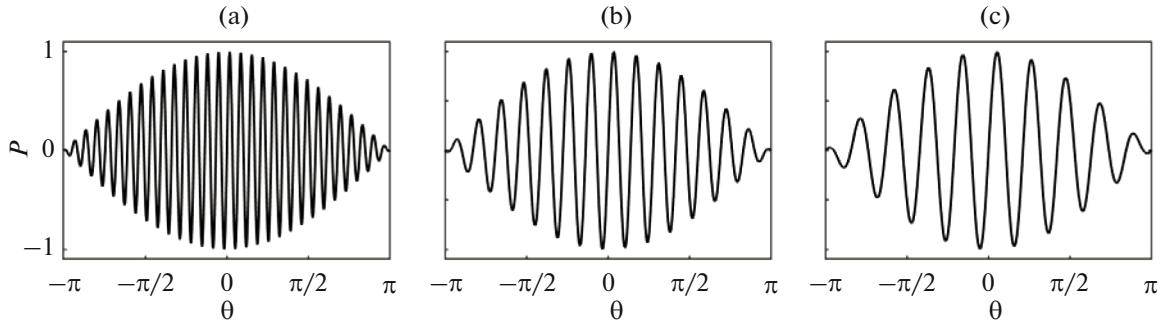


Fig. 1. One period of dimensionless initial pressure waveform at $Z = 0$ for three pairs of interacting pump frequencies: (a) $f_{\text{pump1}} = 150$ kHz and $f_{\text{pump2}} = 145$ kHz, (b) $f_{\text{pump1}} = 150$ kHz and $f_{\text{pump2}} = 140$ kHz, (c) $f_{\text{pump1}} = 150$ kHz and $f_{\text{pump2}} = 135$ kHz.

intensity plane waves that are close in frequency, the Burgers equation can be written as follows [27]:

$$\frac{\partial p}{\partial z} = \frac{\beta}{c_0^3 \rho_0} p \frac{\partial p}{\partial \tau} + \frac{\delta}{2c_0^3} \frac{\partial^2 p}{\partial \tau^2}, \quad (3)$$

with the following boundary condition for the pump waves with frequencies f_{pump1} and f_{pump2} :

$$p(\tau, z = 0) = \frac{p_0}{2} \sin(\omega_{\text{pump1}}\tau) + \frac{p_0}{2} \sin(\omega_{\text{pump2}}\tau), \quad (4)$$

where p_0 is the maximum acoustic pressure reached in the initial pump wave, and $\omega_{\text{pump1}} = 2\pi f_{\text{pump1}}$ and $\omega_{\text{pump2}} = 2\pi f_{\text{pump2}}$ are the angular frequencies.

For convenience of obtaining the numerical solution of the Eq. (3), the dimensionless variables were introduced: $P = p/p_0$, $\theta = \omega_{\text{dif}}\tau$, $Z = z/l_{\text{sh}}$, where $\omega_{\text{dif}} = 2\pi f_{\text{dif}}$ is the angular frequency corresponding to the difference frequency $f_{\text{dif}} = f_{\text{pump1}} - f_{\text{pump2}}$ (for definiteness we set $f_{\text{pump1}} > f_{\text{pump2}}$), l_{sh} is the shock formation distance for the wave cycle with maximum amplitude p_0 and frequency ω_{pump1} , which is the k th harmonic of the difference frequency ($\omega_{\text{pump1}} \equiv \omega_k = k\omega_{\text{dif}}$):

$$l_{\text{sh}} = \frac{\rho_0 c_0^3}{\beta \omega_{\text{pump1}} p_0}.$$

In addition, introducing the inverse acoustic Reynolds number, or Goldberg number Γ , at the pump frequency f_{pump1} as

$$\Gamma = \frac{\delta \omega_{\text{pump1}} \rho_0}{2\beta p_0}, \quad (5)$$

the Burgers equation (3) and the boundary condition (4) can be rewritten in the dimensionless form as:

$$\frac{\partial P}{\partial Z} = \frac{1}{k} \left(P \frac{\partial P}{\partial \theta} + \frac{\Gamma}{k} \frac{\partial^2 P}{\partial \theta^2} \right), \quad (6)$$

$$P(\theta, Z = 0) = 0.5(\sin(k\theta) + \sin([k-1]\theta)). \quad (7)$$

Equation (3) with boundary condition (4) has an analytical solution for the amplitude $A_{\text{dif,analyt}}(z)$ of a difference-frequency wave in a quasi-linear approxi-

mation assuming constant amplitudes A_1 and A_2 (4) of the pump waves [28]:

$$A_{\text{dif,analyt}}(z) = \frac{\beta}{2c_0^3 \rho_0} \omega_{\text{dif}} A_1 A_2 z. \quad (8)$$

1.2. Boundary Wave Field and Parameters of the Medium

Numerical simulation of the generation and propagation of a difference-frequency wave was performed here using frequencies, amplitudes, and parameters of the medium typical for experiments with a recently developed parametric underwater array [29]. It has been assumed that the maximum efficiency of the parametric array is attained at a sufficiently high intensity of the pump waves, when the nonlinear effects balance dissipative processes and the acoustic waveform is distorted being close to contain a shock front [30, 31]. For numerical analysis, as the boundary condition, three pump waves with frequencies $f_{\text{pump1}} = 150$ kHz and $f_{\text{pump2}} = 145, 140,$ and 135 kHz were considered. Hence, the difference-frequency waves were generated at the frequencies $f_{\text{dif}} = 5, 10,$ and 15 kHz, respectively. Figure 1 shows one period of the initial dimensionless pressure waveforms used as a boundary condition (7) to the modeling for three selected pairs of interacting pump frequencies.

To estimate the relative contributions of nonlinearity and absorption, the data of recent experimental studies with an underwater parametric array were used: $p_0 = 0.6$ MPa, $c_0 = 1502.25$ m/s, $\rho_0 = 996.81$ kg/m³ [29]; and nonlinear and absorption parameters typical for seawater: $\beta = 3.5$, $\delta = 4.42 \times 10^{-6}$ m²/s [32].

1.3. Numerical Algorithm

We represent the solution to the Eq. (6) in the form of a finite Fourier series with number N_{max} of the temporal harmonics

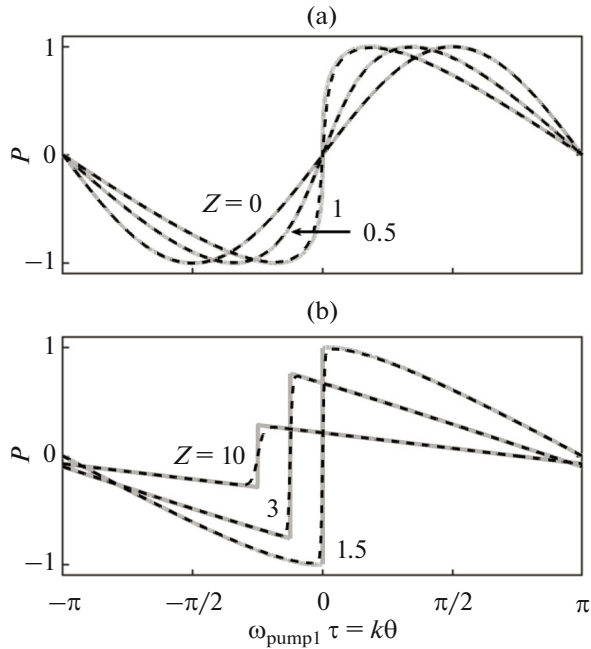


Fig. 2. Distortion of one period of dimensionless pressure waveform of the pump wave with frequency $f_{\text{pump1}} = 150$ kHz, amplitude p_0 , and absorption $\Gamma_{\text{model}} = 0.01$ at distances: (a) $Z = 0, 0.5$, and 1 , showing gradual steepening of the waveform prior to the shock front formation; (b) $Z = 1.5, 3$, and 10 , after shock is formed and the wave amplitude decreases with the propagation distance. Waveforms at distances $Z = 3$ and $Z = 10$ are artificially shifted along the time scale by $\pi/8$ and $\pi/4$, respectively. Solid curve is the analytical solution, dashed curve is the numerical solution obtained for $N_{\text{max}} = 250$ spectral harmonics.

$$P(\theta, Z) = \sum_{n=-N_{\text{max}}}^{N_{\text{max}}} P_n(Z) e^{in\theta}.$$

Then Eq. (6) is written in the frequency representation as a finite system of coupled nonlinear equations [26]:

$$\frac{\partial P_n}{\partial Z} = \frac{in}{k} \left(\sum_{m=1}^{N_{\text{max}}-n} P_m^* P_{n+m} + \frac{1}{2} \sum_{m=1}^{n-1} P_m P_{n-m} \right) - \frac{\Gamma}{k^2} n^2 P_n, \quad (9)$$

where $1 \leq n \leq N_{\text{max}}$, P_m^* is the complex conjugate amplitude of the m th harmonic and i is the imaginary unit. In this case, the boundary condition (7) is $P_{k-1,0} = P_{k,0} = -0.25i$.

The system of equations (9) was solved using operator-splitting method [16–18], where each step over the coordinate Z started and ended with the absorption operator calculated at a half-step $\Delta Z/2$ of the grid. Thus, the operator-splitting scheme can be represented as follows:

$$P(\theta, Z + \Delta Z) = L_{A,\Delta Z/2} L_{N,\Delta Z} L_{A,\Delta Z/2} P(\theta, Z),$$

where the absorption operator at step $\Delta Z/2$ and the nonlinear operator at step ΔZ are denoted as $L_{A,\Delta Z/2}$

and $L_{N,\Delta Z}$, respectively. The system of nonlinear equations (9) without absorption was solved by the fourth-order Runge–Kutta method [26]. To calculate the absorption of each harmonic, analytical solution in the form of a decaying exponent was used.

To reveal the optimum parameters of the numerical algorithm for obtaining reference solutions, we first calculated the propagation of a plane pump wave with frequency $f_{\text{pump1}} = 150$ kHz and amplitude p_0 , which corresponds to the maximum amplitude in the pressure waveform during the two-frequency interaction (Fig. 1): $p(\tau, z = 0) = p_0 \sin(\omega_{\text{pump1}} \tau)$. Calculations were performed for $N_{\text{max}} = 250$ harmonics, the dimensionless step of the spatial grid $\Delta Z = 0.01$, the Goldberg number (5) $\Gamma = 10^{-3}$. To ensure the stability of the numerical scheme during modeling, it is necessary to provide about 9 points per shock [33] that is determined by corresponding absorption coefficient δ for the selected number of harmonics N_{max} . Therefore, the physical Goldberg number $\Gamma = 10^{-3}$ was increased by about ten times. Selection of $\Gamma_{\text{model}} = 0.01$ was determined by the number of harmonics $N_{\text{max}} = 250$ chosen for modeling and corresponding to the time step of the grid $\Delta \theta = \pi/N_{\text{max}}$. In this case, appreciable discrepancies are only observed in the structure of the shock front in its vicinity $\theta = 0 \pm 4\pi/N_{\text{max}}$, which is 1.6% of the duration of the period.

Figure 2 compares the results of numerical simulations for the above-mentioned parameters (dashed curve) with the analytical solution for a Riemann plane wave [34] (solid curve). Clearly, the numerical solution agrees well with the analytical one both at distances before ($Z < 1$) and after ($Z > 1$) shock formation. Some discrepancies are observed only in the fine structure of the shock front and are due to the finite value of the Goldberg number, which makes it possible to use a limited number of harmonics in simulations. The solutions hardly differ at all in other intervals, and at $\theta = 0 \pm 20\pi/N_{\text{max}}$, the error is already less than 1%. Therefore, the use of 250 harmonics to describe nonlinear processes in a high-frequency wave can be considered as acceptable.

Now, to model two-frequency interactions, we also used 250 harmonics of pump frequency f_{pump1} and Goldberg number $\Gamma_{\text{model}} = 0.01$. In the direct formulation, to describe waves with the selected frequencies $f_{\text{pump1}} = 150$ kHz and $f_{\text{pump2}} = 145, 140$ and 135 kHz, it is necessary to take into account $N_{\text{max}} = 7500, 3750$ and 2500 harmonics of the difference frequency, respectively. This is difficult to implement in the modeling nonlinear-diffraction problems based on the Eqs. (1) and (2) due to the quadratic growth of the number of operations when calculating nonlinear operator (9) as a function of N_{max} .

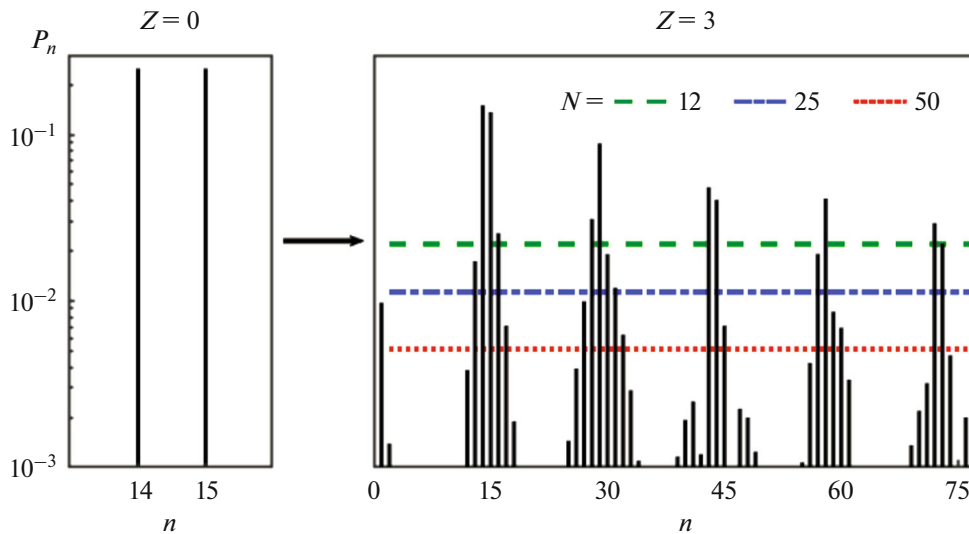


Fig. 3. Illustration to the method of filtering the spectrum by the example of $f_{\text{dif}} = 10$ kHz. The spectrum P_n of the initial wave at the distance $Z = 0$ is shown on the left, where $n = f/f_{\text{dif}}$ is the number of the difference-frequency harmonic; the spectrum at $Z = 3$ and thresholds for $N = 12, 25, 50$ (dashed, dash-dotted and dotted lines, respectively) are shown on the right.

1.4. Filtering the Spectrum

The idea behind the method proposed in this paper for reducing the number of spectral components in the numerical solution, or filtering the spectrum, is as follows. It is known that as a quasi-harmonic high-intensity wave propagates, cascade processes of generating new frequencies are directed mainly towards transition of the wave energy to higher frequencies [27]. The efficiency of the inverse processes towards generation of difference frequencies is extremely lower. Thus, only high-frequency components with the highest amplitudes will mainly contribute to the generation of low-frequency spectral components. These components are concentrated near multiple frequencies of the pump waves. The total spectrum of the nonlinear wave also contains frequencies with sufficiently small amplitudes, which can be omitted without significant loss of accuracy in the solution for the difference-frequency wave. Filtering the spectrum is illustrated in Fig. 3 for $f_{\text{dif}} = 10$ kHz, where the left graph shows the initial wave spectrum at distance $Z = 0$ (two peaks at the pump frequencies), and the right graph shows the wave spectrum at distance $Z = 3$ calculated with the use of the total number of harmonics $N_{\text{max}} = 3750$. Note that the distance $Z = 3$ corresponds to the three shock formation distances for the high-frequency period with maximum amplitude p_0 ; the nonlinear effects for the remaining periods with smaller amplitudes are less pronounced (Fig. 1). Indeed, the amplitudes of the spectral components are the highest near the multiple harmonics of the pump frequencies and much smaller between them.

To determine the numbers of harmonics with the highest amplitudes, we introduced dimensionless threshold pressure P_{th} , which cuts off the harmonics

with lower amplitudes (except for the first harmonic). Thus, the optimized algorithm includes predetermined number of harmonics N which is less than is used in the reference solution. Here, the “reference” solution is the numerical solution obtained by modeling with all harmonics N_{max} . Threshold values P_{th} were varied so that the number of spectral components with amplitudes above the threshold was $N = 12, 25, 50$ (dashed, dash-dotted, and dotted lines, respectively). The dimensionless distance $Z = 1, 1.5, \text{ and } 3$, at which this procedure was performed, was also varied for three values of f_{dif} considered in this work. In the obtained filtered spectrum with amplitudes above the threshold level, first, the high-frequency part of the spectrum was limited, and second, the number of combination components was reduced between the frequencies that are amplitude peaks of the multiples of the pump frequencies f_{pump1} and f_{pump2} . Then, the algorithm for solving Eq. (6) was modified so that the calculations were performed only using the indices of the harmonics retained after filtering.

2. RESULTS AND DISCUSSION

Figure 4 shows the amplitude P_{dif} of a difference-frequency wave along the propagation distance Z for three values of f_{dif} : 5 kHz (Figs. 4a, 4d), 10 kHz (Figs. 4b, 4e), and 15 kHz (Figs. 4c, 4f). The reference solution at $N = N_{\text{max}}$ is shown in all plots by solid red curves, and the quasi-linear solution (8) is shown by the grey marker curve. The upper row of plots (Figs. 4a–4c) was obtained by filtering the spectrum of the reference solution at distance $Z = 3$ with a different number of harmonics included in the nonlinear algorithm: $N = 12$ (dashed curve), 25 (solid curve),

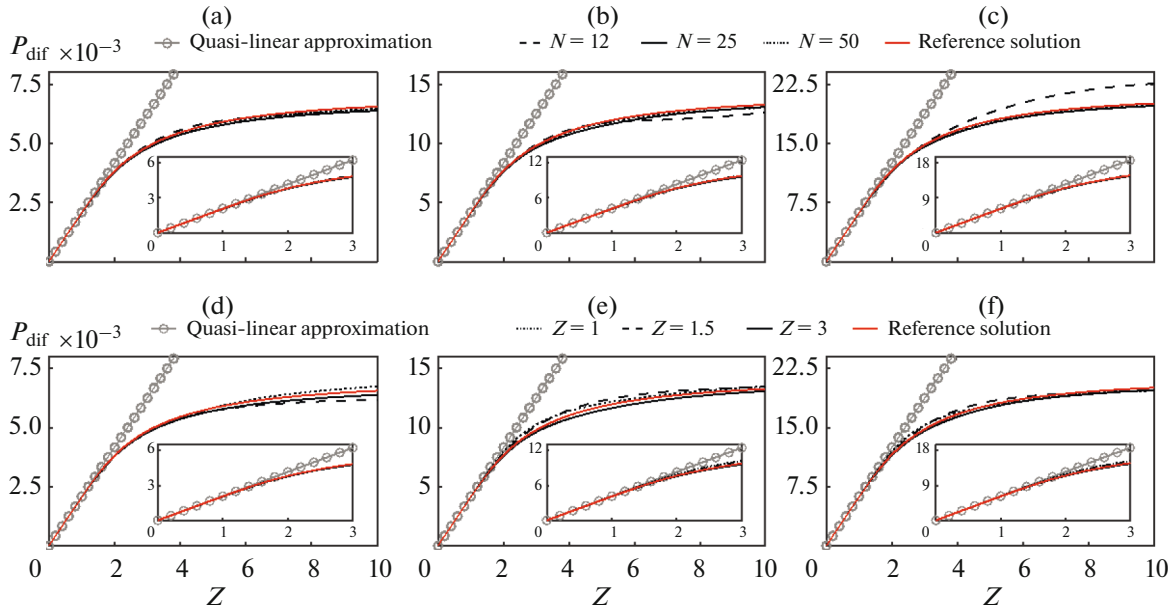


Fig. 4. Dependences of the amplitude P_{dif} of difference-frequency wave on distance Z for three values of f_{dif} : (a, d) 5 kHz, (b, e) 10 kHz, and (c, f) 15 kHz. (a–c) filtering the spectrum at the distance $Z = 3$ with different numbers of harmonics included in the algorithm: $N = 12$ (dashed curve), 25 (solid curve), and 50 (dotted curve); (d–f) filtering the spectrum for $N = 25$ at different distances: $Z = 1$ (dotted curve), 1.5 (dashed curve), and 3 (solid curve). The solution in the quasi-linear approximation (solid marker curve) and the reference solution (solid red curve) for $N = N_{\text{max}}$ (7500, 3750, and 2500) are also shown. Dependences $P_{\text{dif}}(Z)$ at the initial stage of propagation are shown in the insets to the corresponding figures.

and 50 (dotted curve). The lower row (Figs. 4d–4f) was obtained by filtering the spectrum with a constant number of harmonics $N = 25$ included in the nonlinear algorithm, but at different distances: $Z = 1$ (dotted curve), 1.5 (dashed curve), and 3 (solid curve). Dependences $P_{\text{dif}}(Z)$ at the initial stage of propagation are shown in the insets to the corresponding figures.

As shown in the figure, at the initial stage up to the distance $Z = 2$, the amplitude of the difference-frequency wave obtained by the numerical solution both including all harmonics and with the spectrum filtering grows linearly and practically is indistinguishable from the result of the analytical solution obtained in the quasi-linear approximation. Then the linear growth slows down and turns to saturation at distances of the order of several lengths of the shock formation. In this case, the higher difference frequency f_{dif} is, the more energy is transferred to it from the pump frequencies. Thus, according to the quasi-linear approximation (8), at distance $Z = 1$, the amplitude of the difference-frequency wave is proportional to its frequency. For $f_{\text{dif}} = 5$ kHz it is 0.2%, for $f_{\text{dif}} = 10$ kHz it is 0.4%, and for $f_{\text{dif}} = 15$ kHz it is 0.6% of the maximum amplitude p_0 of the initial pump wave. The intensities of the difference-frequency waves are 0.01, 0.04, and 0.09% of the initial intensity $p_0^2/(4c_0\rho_0)$ averaged over the period of a low-frequency wave. At distances of several shock formation lengths, at which the amplitude of the difference-frequency wave

becomes saturated, this amplitude additionally increases more than twofold, which corresponds to a more than fourfold increase in intensity.

Figures 4a–4c show the effect of filtering the spectrum of the reference solution at distance $Z = 3$ on the accuracy of the numerical solution for P_{dif} at different numbers of harmonics $N = 12, 25$, and 50 included in the nonlinear algorithm versus the reference solution at $N = N_{\text{max}}$. For the number of harmonics $N = 12$, the numerical solution for the difference-frequency wave considerably differs from the reference one starting from distances of about $Z = 3$. The use of $N = 25$ harmonics in the nonlinear algorithm results in an error in calculating the amplitude of the difference-frequency wave of less than 0.4% at distance $Z = 1$, less than 1.8% at $Z = 3$, and less than 2.8% at $Z = 10$, while the maximum error over the entire distance range is less than 2.8%. Accounting for $N = 50$ harmonics results in an error not exceeding 2% at all distances. Considering that parametric arrays operate mainly in modes close to the shock front formation, selection of $N = 25$ harmonics seems sufficient for further analysis.

Figures 4d–4f show the results of filtering the spectrum with a constant number of harmonics $N = 25$ included in the nonlinear algorithm at different distances $Z = 1, 1.5$, and 3 versus the reference solution at $N = N_{\text{max}}$. Clearly, all obtained solutions are quite close, but filtering at the distance $Z = 3$ is preferable. This selection results in an error which is less than

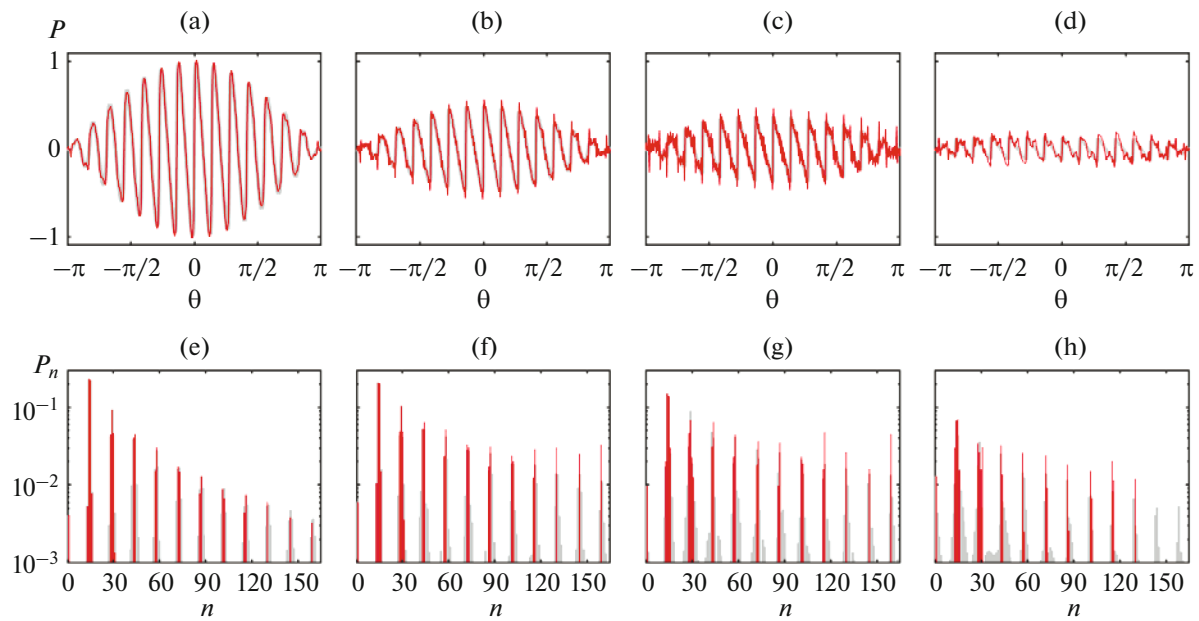


Fig. 5. (a–d) One period of dimensionless pressure waveform for $f_{\text{pump}1} = 150$ kHz and $f_{\text{pump}2} = 140$ kHz at distances $Z = 1, 1.5, 3$, and 10 , respectively; (e–h) wave spectrum at the same distances $Z = 1, 1.5, 3$, and 10 , respectively. The reference solution is shown by the bold grey curve, the result of filtering the spectrum at distance $Z = 3$ by including $N = 25$ harmonics in the nonlinear algorithm is shown by the thin red curve.

2.8% compared to the reference solution at all distances for all three difference frequencies.

Thus, for three pairs of interacting pump waves with difference frequencies $f_{\text{dif}} = 5, 10$, and 15 kHz, the number of spectral components included in the nonlinear algorithm can be reduced from $N_{\text{max}} = 7500, 3750$, and 2500 to $N = 25$. The error in calculating the amplitude of the difference-frequency wave is less than 3% with the most appropriate selection of the distance at which filtering of the spectrum is performed. Further results will be presented for $N = 25$ spectral components obtained by filtering the reference numerical solution at the distance $Z = 3$.

Note that at distances $Z < 2$, the analytical solution (8) obtained in the quasi-linear approximation for constant pump wave amplitudes (solid marker curve in Figs. 4a–4f) agrees well with the reference solution and can be used instead of numerical calculation of the nonlinear operator. At distances $Z > 2$, the error associated with using the quasi-linear approximation rapidly increases.

Figure 5 shows typical pressure waveforms (Figs. 5a–5d) and spectra (Figs. 5e–5h) obtained by filtering the reference spectrum at the distance $Z = 3$ and selecting the threshold at which $N = 25$, for $f_{\text{dif}} = 10$ kHz when the wave propagates over distances $Z = 1, 1.5, 3$, and 10 (fine red curve) versus the reference solution for $N = N_{\text{max}}$ (bold gray curve). As seen from the figure, fluctuations in the pressure waveform occur due to the effect of frequency reflection due to the limitation of retained high-frequency harmonics

(Figs. 5a–5d). However, as shown above, these artifacts in the description of the total spectrum of the wave weakly affect the amplitude of the difference-frequency wave (Fig. 4). The final filtered spectrum (Figs. 5e–5h) contains the difference-frequency component and groups of one to five spectral components around 11 peaks, which are multiples of the initial pump frequencies. Each of these groups is a successive alternation of two and one spectral components with the maximum amplitude, on the sides of which combination frequencies are observed. The number of these frequencies varies from 0 to 3 for the first six groups and is zero from the seventh group on.

CONCLUSIONS

In this paper, numerical methods were used to study generation of a difference-frequency wave formed during the interaction of two high-intensity pump waves with close frequencies in a nonlinear medium. The calculations were performed for a one-dimensional wave using the example of three pairs of interacting frequencies typical of the operation of parametric sources in underwater acoustics.

A method for filtering of the wave spectrum was proposed, which made it possible to reduce the number of spectral components included in the nonlinear algorithm by more than two orders of magnitude, thereby reducing the number of operations by four orders of magnitude. The method includes limiting the number of high-frequency components and reducing the combination frequencies with small

amplitude located in the intervals between the harmonics, which are multiples of the initial waves. It is shown that filtering of frequencies in the numerical solution with a large number of spectral components is preferably performed at a distance equal to three shock formation lengths for the high-frequency period of the pump wave with the maximum amplitude. This selection results in an error less than 3% in the calculation of the difference-frequency wave amplitude compared to the calculations with the total number of spectral components up to distances of ten shock formation lengths.

The amplitude of the difference-frequency wave is proportional to its frequency f_{dif} and at a distance equal to one shock formation length it is 0.2, 0.4, and 0.6% of the maximum amplitude of the pump wave or 0.01, 0.04, and 0.09% of the initial intensity averaged over the period of a low-frequency wave for frequencies $f_{\text{dif}} = 5, 10, \text{ and } 15 \text{ kHz}$. At saturation distances, the amplitude and intensity of the difference-frequency wave additionally increase by more than two and four times, respectively.

We have also shown that at distances less than two characteristic shock formation lengths, the analytical expression obtained in the quasi-linear approximation at constant pump wave amplitudes agrees with good accuracy with the reference solution obtained with a large number of spectral components. Therefore, the quasi-linear approximation can be used in modeling nonlinear beams. The results obtained in this study can be subsequently used to solve the complete three-dimensional nonlinear-diffraction problem of generating a difference-frequency wave using a parametric array [29, 31].

FUNDING

This study was supported by the Russian Foundation for Basic Research (project no. 20-02-00676) and by the BASIS Foundation (project no. 20-2-2-21-1).

CONFLICT OF INTEREST

The authors declare no conflicts of interest.

REFERENCES

- W.-S. Gan, J. Yang, and T. Kamakura, *Appl. Acoust.* **73** (12), 1211 (2012).
- H. Zhou, S. H. Huang, and W. Li, *Sensors* **20** (7), 2148 (2020).
- P. J. Westervelt, *J. Acoust. Soc. Am.* **35** (4), 535 (1963).
- B. K. Novikov and V. I. Timoshenko, *Parametric Antennas in Hydro-Location* (Sudostroenie, Leningrad, 1990) [in Russian].
- O. A. Sapozhnikov, V. A. Khokhlova, R. O. Cleveland, P. Blanc-Benon, and M. F. Hamilton, *Acoust. Today* **15** (3), 55 (2019).
- B. K. Novikov, O. V. Rudenko, and V. I. Timoshenko, *Nonlinear Underwater Acoustics* (AIP Publ., 1987).
- V. A. Zverev and A. I. Kalachev, *Sov. Phys. Acoust.* **4** (4), 331 (1958).
- V. A. Zverev and A. I. Kalachev, *Sov. Phys. Acoust.* **14** (2), 214 (1968).
- S. N. Gurbatov, M. S. Deryabin, D. A. Kas'yanov, and V. V. Kurin, *Acoust. Phys.* **63** (3), 260 (2017).
- M. B. Bennett and D. T. Blackstock, *J. Acoust. Soc. Am.* **57** (3), 562 (1975).
- M. Yoneyama, J. Fujimoto, Y. Kawamo, and S. Sasabe, *J. Acoust. Soc. Am.* **73** (5), 1532 (1983).
- C. Shi and W.-S. Gan, *IEEE Potentials* **29** (6), 20 (2010).
- H. Nomura, C. M. Hedberg, and T. Kamakura, *Appl. Acoust.* **73** (12), 1231 (2012).
- L. Zhu and D. Florencio, in *Proc. IEEE Int. Conf. on Acoustics, Speech and Signal Processing (ICASSP)* (IEEE, 2015), p. 5982.
- M. Cervenka and M. Bednarik, *J. Acoust. Soc. Am.* **134** (2), 933 (2013).
- J. Tavakkoli, D. Cathignol, R. Souchon, and O. A. Sapozhnikov, *J. Acoust. Soc. Am.* **104** (4), 2061 (1998).
- P. V. Yuldashev and V. A. Khokhlova, *Acoust. Phys.* **57** (3), 334 (2011).
- R. J. Zemp, J. Tavakkoli, and R. S. C. Cobbold, *J. Acoust. Soc. Am.* **113** (1), 139 (2003).
- F. Prieur, *AIP Conf. Proc.* **1474** (1), 387 (2012).
- Y. S. Lee and M. F. Hamilton, *J. Acoust. Soc. Am.* **97** (2), 906 (1995).
- S. I. Aanonsen, *Tech. Rep. No. 73* (Dept. of Math., Univ. of Bergen, 1983).
- P. Ji, E.-L. Tan, W.-S. Gan, and J. Yang, *IEEE Trans. Audio Speech Lang. Process.* **19** (4), 937 (2011).
- M. A. Averkiou, Y.-S. Lee, and M. F. Hamilton, *J. Acoust. Soc. Am.* **94** (5), 2876 (1993).
- T. Kamakura, N. Hamada, K. Aoki, and Y. Kumamoto, *J. Acoust. Soc. Am.* **85** (6), 2331 (1989).
- T. Kamakura, H. Nomura, M. Akiyama, and C. M. Hedberg, *Acta Acust.* **97** (2), 209 (2011).
- S. S. Kashcheeva, O. A. Sapozhnikov, V. A. Khokhlova, M. A. Averkiou, and L. A. Cram, *Acoust. Phys.* **46** (2), 170 (2000).
- O. V. Rudenko and S. I. Soluyan, *Theoretical Foundations of Nonlinear Acoustics* (Springer, New York, 2013).
- B. K. Novikov, O. V. Rudenko, and S. I. Soluyan, *Sov. Phys. Acoust.* **21** (4), 591 (1975).
- I. B. Esipov, O. E. Popov, and V. G. Soldatov, *Acoust. Phys.* **65** (4), 391 (2019).
- M. B. Moffett, R. H. Mellen, and W. L. Konrad, *J. Acoust. Soc. Am.* **63** (5), 1326 (1978).
- I. B. Esipov, O. E. Popov, G. V. Kenigsberger, and I. I. Sizov, *Bull. Russ. Acad. Sci., Phys.* **80** (10), 1209 (2016).
- A. D. Pierce, *Acoustics: An Introduction to Its Physical Principles and Applications* (Springer, 2019).
- A. D. Maxwell, P. V. Yuldashev, W. Kreider, T. D. Khokhlova, G. R. Schade, T. L. Hall, O. A. Sapozhnikov, M. R. Bailey, and V. A. Khokhlova, *IEEE Trans. Ultrason., Ferroelectr. Freq. Control* **64** (10), 1542 (2017).
- S. N. Gurbatov, O. V. Rudenko, and A. I. Saichev, *Waves and Structures in Nonlinear Nondispersive Media* (Springer, 2011).

Translated by N. Podymova